Electronic Supplementary Material (ESI) for CrystEngComm.
This journal is © The Royal Society of Chemistry 2023

Electronic Supplementary Information (ESI):

Di-triazole boat conformation leads to metal-organic nanotube while chair conformation leads to coordination polymer

Phattananawee Nalaoh and David M. Jenkins*

Department of Chemistry, University of Tennessee, Knoxville, Tennessee 37996, USA

Table of Contents

I. Experimental section

General Procedure

The compound 1,2,4-triazole-1-propanenitrile was synthesized as previously described.[1] All other reagents were purchased from commercial vendors and used without purification.

^{1}H, $^{13}C\{^{1}H\}$, and $^{19}F\{^{1}H\}$ NMR spectra were obtained at 25 °C on a Bruker AVANCE NEO 500 MHz system in $CDCl_3$ and DMSO-d_6. Chemical shifts were referenced to the residual solvent peak for ^{1}H and ^{13}C NMR experiments, while an external reference was used for ^{19}F experiments with trifluoroacetic acid in $CDCl_3$, and DMSO-d_6. High resolution mass spectrometry (HRMS) was analyzed at the Biological and Small Molecule Mass Spectrometry Core Facility located in the Department of Chemistry at the University of Tennessee. LDI-TOF MS was analyzed by Waters Synapt G2-Si MALDI mass spectrometer with a quadrupole time-of-flight mass analyzer. ESI-HRMS was analyzed by a Waters Synapt G2-Si mass spectrometer with a quadrupole time-of-flight mass analyzer operating in electrospray ionization mode. Each sample was introduced to the instrument *via* direct injection. Fourier-transform infrared spectra (FTIR) were analyzed neat on a Thermo Scientific Nicolet iS10 with a Smart iTR accessory for attenuated total reflectance (ATR).

Single crystal analysis: Single crystal structures were determined by a Bruker D8 Venture diffractometer with PHOTON II CPAD detector and employing the use of Mo Kα radiation (λ = 0.71073 Å) at 100 K, where all crystals were mounted on loops (MitiGen®) with Paratone-N (Hampton Research).

PXRD Analysis: XRD patterns were obtained on a PANalytical Empyrean Powder Diffractometer in reflectance Bragg-Brentano geometry with Cu Kα radiation (λ = 1.5406 Å; 1,800 W, 45 kV, 40 mA) on a zero-background silicon plate fixed in a sample holder with a revolution spin rate of 4 s at room temperature. The formation of preferred crystals was verified by comparing its PXRD pattern to the simulated pattern based on the SCXRD data.

Synthesis and characterization

Synthesis of (*trans*-cyclohexane-1,4-diyl)bis(methylene) bis(trifluoromethanesulfonate), 2-1

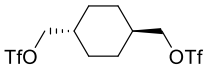

The reaction is adapted from the previously reported procedure of sulfonate ester synthesis.[2] *Trans*-1,4-cyclohexanedimethanol (5.00 g, 34.7 mmol) was dissolved in the mixture of 75 mL dichloromethane and 5 mL pyridine at 0 °C, followed by slowly addition of 50 mL (298 mmol) trifluoromethanesulfonic anhydride for 30 minutes with vigorous stirring. The reaction remained at 0 °C for 30 minutes then warmed to room temperature and left the reaction stirred overnight. After that, the reaction was quenched with water (200 mL) and extracted using dichloromethane (100 mL × 3 times). The organic phase was separated and dried over anhydrous sodium sulfate. The solvent was removed under vacuum which obtained pale-white solid crystals.

Yield 12.3 g, 87%.

^{1}H NMR (500 MHz, $CDCl_3$): δ 4.36 (d, *J* = 6.2 Hz, 8H), 2.00 – 1.87 (m, 8H), 1.87 – 1.76 (m, 4H), 1.23 – 1.05 (m, 8H).

$^{13}C\{^{1}H\}$ NMR (126 MHz, $CDCl_3$): δ 118.81 (q, *J* = 319.7 Hz), 81.17, 37.29, 27.70.

$^{19}F\{^{1}H\}$ NMR (471 MHz, $CDCl_3$): δ -74.62.

IR (neat): 2956, 2931, 2864, 1472, 1464, 1450, 1402, 1390, 1381, 1272, 1242, 1194, 1143, 1029, 961, 941, 924, 838, 828, 764 cm^{-1}.

Synthesis of 4,4'-((*trans*-cyclohexane-1,4-diyl)bis(methylene))bis(1-(2-cyanoethyl)-4H-1,2,4-triazol-1-ium) triflate, 2-2

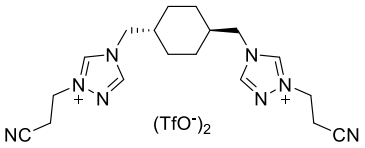

Compound **2-1** (4.08 g, 10.0 mmol) and protected triazole, 3-(1*H*-1,2,4-triazol-1-yl)propanenitrile (2.68 g, 22.0 mmol) were dissolved in 30 mL acetonitrile, followed by refluxing for 24 hours under a nitrogen atmosphere. White solid appeared in the flask after 12 h of the reaction. After cooling down, the mixture was filtered and washed with acetonitrile, which yielded the desired product **2-2** as white solid.

Yield 6.00 g, 92%.

^{1}H NMR (500 MHz, DMSO-d_6): δ 10.16 (s, 2H), 9.29 (s, 2H), 4.71 (t, *J* = 6.3 Hz, 4H), 4.19 (d, *J* = 7.1 Hz, 4H), 3.22 (t, *J* = 6.3 Hz, 4H), 1.86 – 1.73 (m, 2H), 1.66 (d, *J* = 8.0 Hz, 4H), 0.98 (td, *J* = 8.9, 3.2 Hz, 4H).

$^{13}C\{^{1}H\}$ NMR (126 MHz, DMSO-d_6): δ 145.29, 143.36, 117.65, 52.67, 47.17, 36.93, 28.11, 17.40.

$^{19}F\{^{1}H\}$ NMR (471 MHz, DMSO-d_6): δ -77.72.

HRMS (MALDI-TOF) m/z: $[M]^+$ Calcd for $C_{19}H_{26}F_3N_8O_3S$ 503.1795; Found 503.1801.

IR (neat): 3125, 3041, 2947, 2254, 1575, 1528, 1458, 1414, 1394, 1357, 1254, 1225, 1155, 1072, 1051, 1027, 1005, 990, 958, 932, 918, 908, 825, 758, 750, 650, 630 cm^{-1}.

Synthesis of *trans*-1,4-bis((4H-1,2,4-triazol-4-yl)methyl)cyclohexane, L2

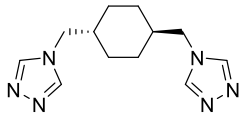

Compound **2-2** (1.00 g, 1.53 mmol) was dissolved in 15% w/v NH_4OH solution (20 mL) and stirred at room temperature for 24 hours. The solution was then condensed *in vacuo*, which gave a yellow oil. 2-propanol (20 mL) was added to the crude product as an antisolvent for recrystallization, which yielded white solid crystals of the product.

Yield 0.140 g, 37%.

^{1}H NMR (500 MHz, DMSO-d_6) δ 8.46 (s, 4H), 3.87 (d, *J* = 7.0 Hz, 4H), 1.62 (s, 2H), 1.57 – 1.46 (m, 4H), 0.89 (td, *J* = 8.9, 3.2 Hz, 4H).

^{13}C{^{1}H} NMR (126 MHz, DMSO-d_6) δ 143.50, 49.76, 37.97, 28.75.

HRMS (MALDI-TOF) m/z: $[M + Na]^+$ Calcd for $C_{12}H_{18}N_6Na$ 269.1485; Found 269.1507.

IR (neat): 3115, 3082, 2923, 2856, 1707, 1538, 1527, 1462, 1372, 1341, 1314, 1290, 1269, 1220, 1187, 1181, 1081, 1072, 974, 953, 931, 892, 864, 830, 728, 683, 642 cm^{-1}.

Synthesis of bicyclo[2.2.2]octane-1,4-dicarboxamide, 3-1

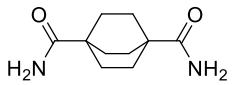

The synthesis of compound **3-1** was adapted from a previously published amide synthesis from carboxylic acid.[3] Bicyclo[2.2.2]octane-1,4-dicarboxylic acid (2.08 g, 10.5 mmol) were suspended in 50 mL of dry dichloromethane at room temperature. Then, 2.25 mL (26.2 mmol) of oxalyl chloride was slowly added to the reaction mixture, followed by addition of 0.2 mL *N*,*N*-dimethylformamide to initiate the formation of acyl chloride intermediate. After the reaction was left at room temperature for 2 hours, the solvent residue was removed under the reduced pressure. The crude product, which has a yellow sticky wax appearance, had *conc.* NH_4OH (10 mL) slowly added to it which generated heat and white smoke. The reaction was left at room temperature for 30 minutes with a white solid appeared in the reaction. The solid was filtered over filter paper and washed with deionized water to remove all water-soluble residue and then dried at 110 °C to remove water, obtaining compound **3-1** as white solid powder.

Yield 1.44 g, 69%.

^{1}H NMR (500 MHz, DMSO-d_6): δ 6.91 (s, 2H), 6.67 (s, 2H), 1.62 (s, 12H).

^{13}C{^{1}H} NMR (126 MHz, DMSO-d_6): δ 178.95, 37.87, 27.91.

HRMS (ESI) m/z: $[M+H]^+$ Calcd for $C_{10}H_{17}N_2O_2$ 197.1290; Found 197.1298.

IR (neat): 3390, 3166, 2953, 2920, 2871, 2776, 1658, 1623, 1598, 1460, 1392, 1316, 1294, 1167, 1142, 1120, 1094, 981, 846, 826, 721, 692, 626, 532 cm^{-1}.

Synthesis of bicyclo[2.2.2]octane-1,4-diyldimethanamine, 3-2

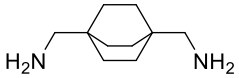

Compound **3-1** (1.30 g, 6.62 mmol) was suspended in 50 mL dried THF, followed by addition of $LiAlH_4$ (2.00 g, 53.0 mmol) in three portions. The reaction mixture was heated at reflux for 6 hours under a nitrogen atmosphere. After the reaction was cooled down to room temperature, 1 M KOH solution (30 mL) was added to quench the reaction, and a white solid appeared. The solid residue was filtered through the fritted glass funnel. The filtrate was extracted with dichloromethane (3 × 50 mL) and then brine solution. The organic phase was separated, dried over anhydrous $MgSO_4$, and removed the solvent under reduced pressure to obtain compound **3-2** as a yellow oil.

Yield 0.403 g, 36%.

^{1}H NMR (500 MHz, DMSO-d_6): δ 2.20 (s, 4H), 1.27 (s, 12H).

^{13}C{^{1}H} NMR (126 MHz, DMSO-d_6): δ 51.94, 32.90, 28.56.

HRMS (ESI) m/z: $[M+H]^+$ Calcd for $C_{10}H_{21}N_2$ 169.1705; Found 169.1712.

IR (neat): 3371, 3294, 2912, 2852, 1667, 1601, 1454, 1374, 1260, 1160, 1043, 864, 819, 732, 713, 644, 566, 542, 532 cm^{-1}.

Synthesis of 1,4-bis((4H-1,2,4-triazol-4-yl)methyl)bicyclo[2.2.2]octane, L3

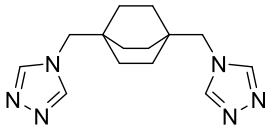

Compound **3-2** (336 mg, 1.0 mmol), *N*,*N*'-Bis(dimethylaminomethylene)hydrazine (355 mg, 2.5 mmol), and p-toluenesulfonic acid (35 mg, 0.2 mmol) were dissolved in 20 mL *o*-xylene. The reaction mixture was heated at reflux for 16 h. After the reaction was cooled down to room temperature, all solid residue was decanted and washed with toluene (20 mL) three times. The solid residue was crystallized in hot 2-propanol (10 mL) to obtain an off-white solid powder of **L3**.

Yield 0.240 g, 50%.

^{1}H NMR (500 MHz, DMSO-d_6) δ 8.39 (s, 4H), 3.76 (s, 4H), 1.27 (s, 12H).

^{13}C{^{1}H} NMR (126 MHz, DMSO-d_6) δ 144.02, 53.08, 32.13, 27.87.

HRMS (ESI) m/z: $[M + Na]^+$ Calcd for $C_{14}H_{20}N_6Na$ 295.1647; Found 295.1649.

IR (neat): 3107, 2935, 2916, 2860, 1698, 1530, 1455, 1444, 1432, 1366, 1335, 1315, 1184, 1121, 1076, 1034, 1011, 977, 953, 862, 823, 729, 686, 633, 565 cm^{-1}.

General procedure for MONT and coordination polymers synthesis. The synthesis of the MONT and coordination polymer was adapted the previously published processes.[4] Solutions of **L2** or **L3** were prepared in *N*-methyl-2-pyrrolidone (NMP). Meanwhile, a solution of $AgNO_3$ was dissolved in H_2O. All solution vials were heated in an aluminum heating block at 85 °C for 30 minutes. Then, each ligand and metal salt solutions were mixed in the separate vials and heated at 85 °C for 24 hours. This step generally provided MONT or coordination polymer crystals which were removed from the bulk product, washed with methanol and water, and dried over air for XRD analysis and characterization.

Synthesis of Ag(L2)(NO_3)

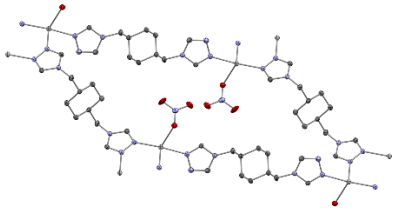

L2 (49.2 mg, 0.20 mmol), $AgNO_3$ (67.9 mg, 0.40 mmol), H_2O (10.0 mL), NMP (10.0 mL) were used.

White solid crystal (45.2 mg, 54% yield).

IR (neat): 3090, 2920, 2850, 1545, 1533, 1472, 1450, 1377, 1320, 1263, 1246, 1192, 1166, 1087, 1079, 1065, 1041, 1010, 982, 970, 956, 906, 872, 826, 730, 720, 683, 651, 627 cm^{-1}.

Elemental analysis (%): Calcd. for $C_{12}H_{18}AgN_7O_3$: C = 34.63; H = 4.36; N = 23.56. Found: C = 34.36; H = 4.32; N = 23.37.

Synthesis of Ag_2(L3)(NO_3)$_2$

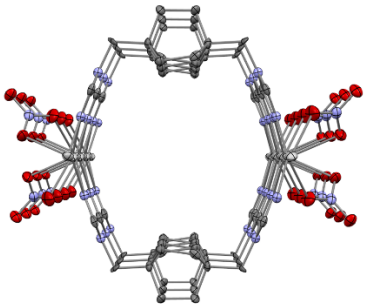

L3 (50.0 mg, 0.20 mmol), $AgNO_3$ (67.9 mg, 0.40 mmol), H_2O (10.0 mL), NMP (10.0 mL) were used.

Off-white solid crystal (42.6 mg, 35% yield).

IR (neat): 3092, 3059, 3002, 2940, 2865, 1694, 1675, 1544, 1439, 1370, 1317, 1262, 1225, 1199, 1083, 1022, 911, 864, 820, 798, 720, 690, 653, 636, 596, 580, 571, 563, 556 cm^{-1}.

Elemental analysis (%): Calcd. for $C_7H_{10}AgN_4O_3$ • 0.33 (C_5H_9NO): C = 30.70; H = 3.86; N = 17.90. Found: C = 30.55; H = 3.37; N = 16.71.

^{1}H, ^{13}C, ^{19}F, and FTIR Spectra

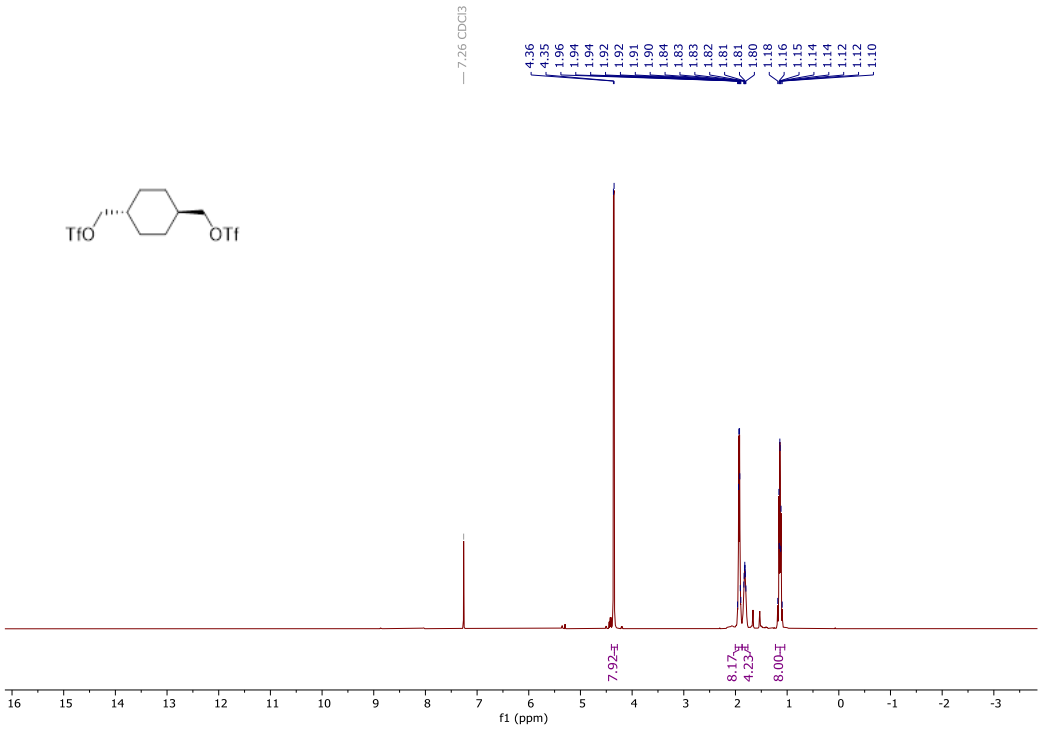

Fig. S1. ^{1}H NMR spectrum of (*trans*-cyclohexane-1,4-diyl)bis(methylene) bis(trifluoromethanesulfonate), **2-1**, in $CDCl_3$

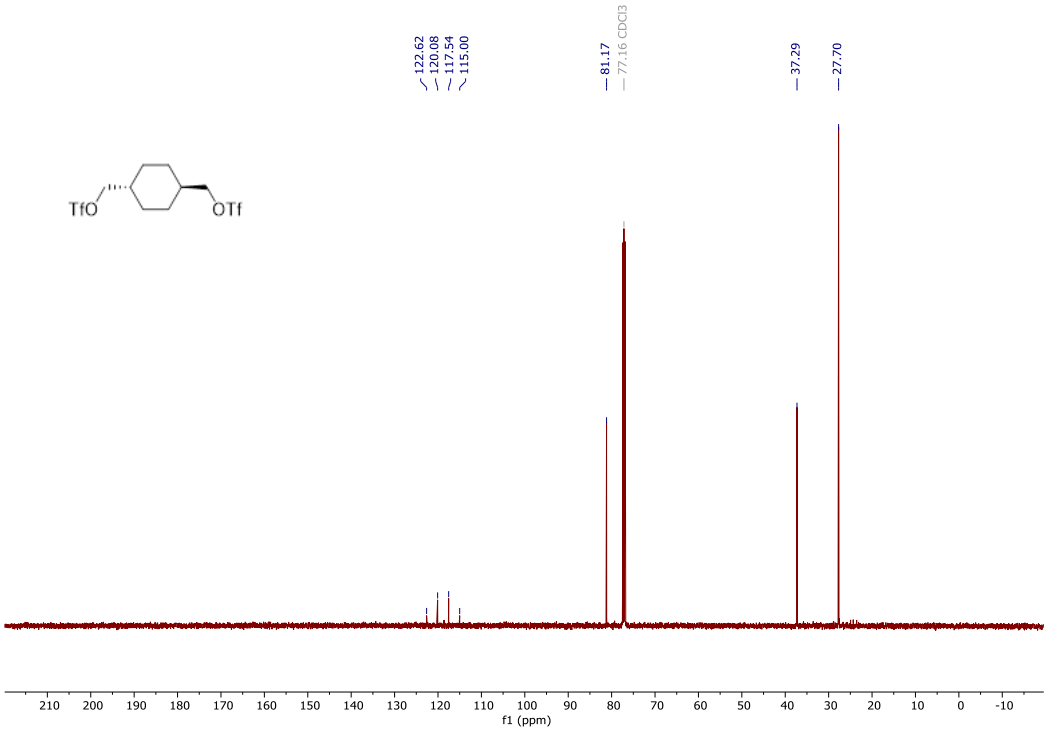

Fig. S2. ^{13}C NMR spectrum of (*trans*-cyclohexane-1,4-diyl)bis(methylene) bis(trifluoromethanesulfonate), **2-1**, in $CDCl_3$

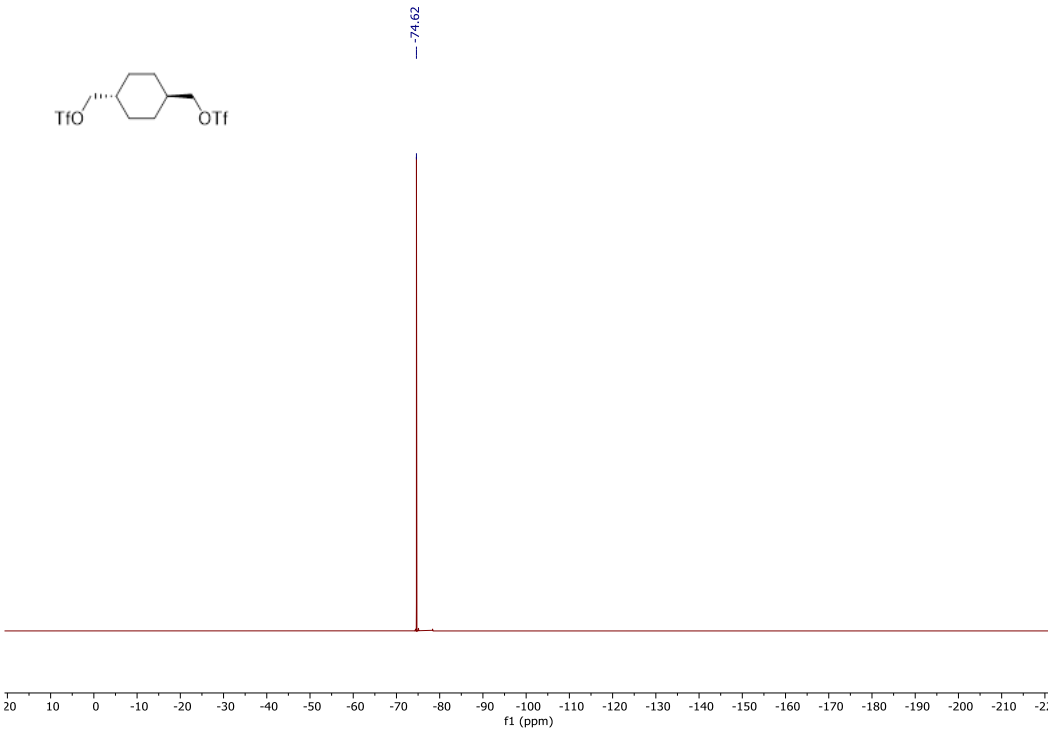

Fig. S3. ^{19}F NMR spectrum of (*trans*-cyclohexane-1,4-diyl)bis(methylene) bis(trifluoromethanesulfonate), **2-1**, in $CDCl_3$

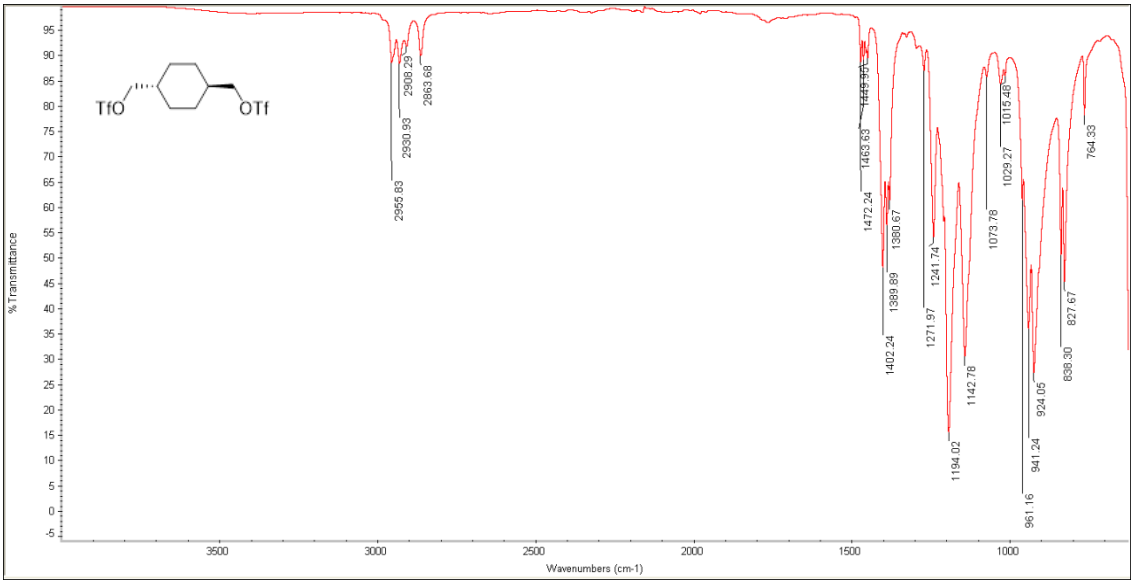

Fig. S4. IR spectrum of (*trans*-cyclohexane-1,4-diyl)bis(methylene) bis(trifluoromethanesulfonate), **2-1**

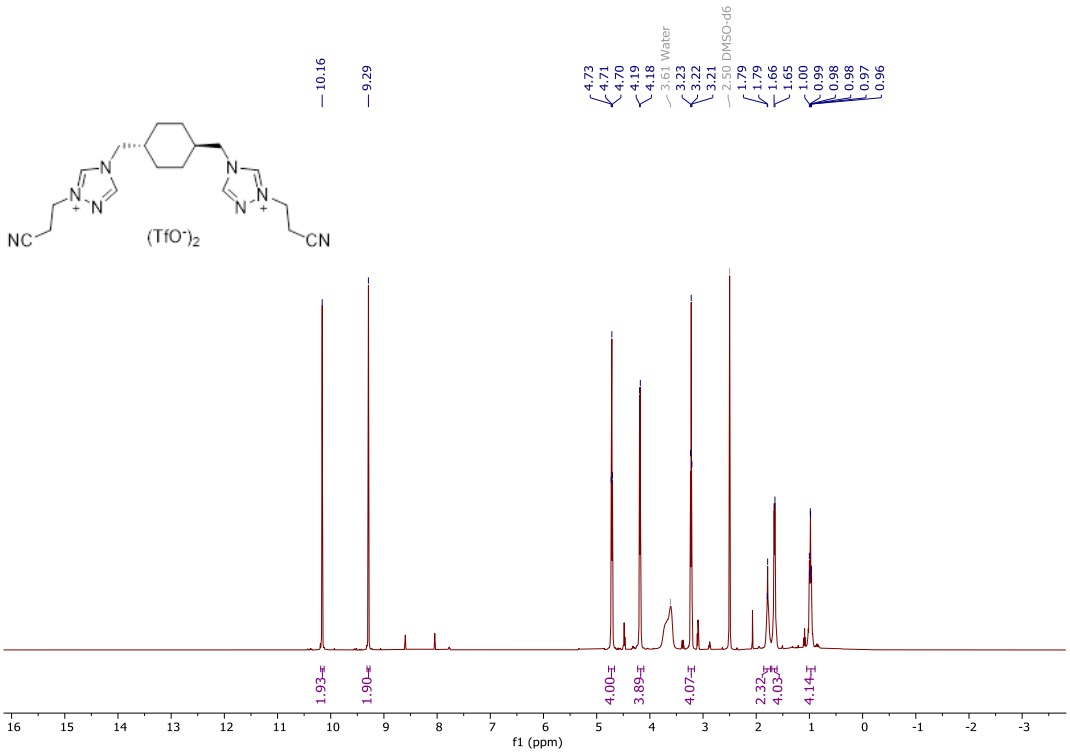

Fig. S5. ^{1}H NMR spectrum of 4,4'-((*trans*-cyclohexane-1,4-diyl)bis(methylene))bis(1-(2-cyanoethyl)-4*H*-1,2,4-triazol-1-ium) triflate**, 2-2**, in DMSO-d_6, which contains less than 5% 3-(1*H*-1,2,4-triazol-1-yl)propanenitrile as an impurity.

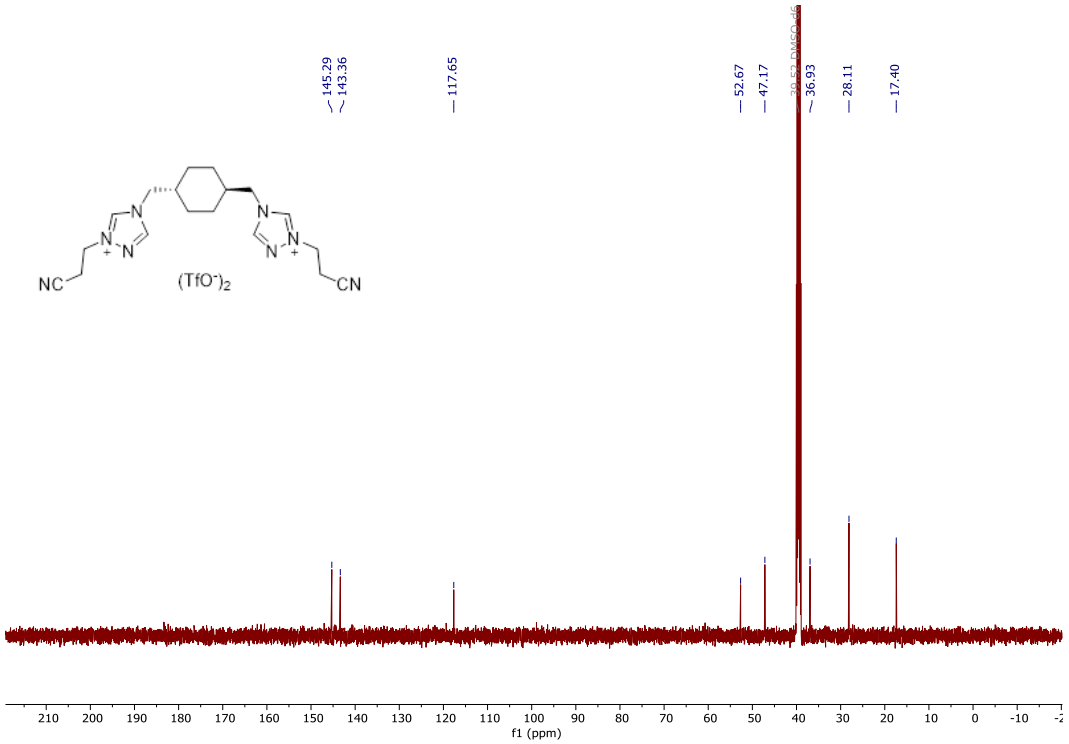

Fig. S6. ^{13}C NMR spectrum of 4,4'-((*trans*-cyclohexane-1,4-diyl)bis(methylene))bis(1-(2-cyanoethyl)-4*H*-1,2,4-triazol-1-ium) triflate**, 2-2**, in DMSO-d_6

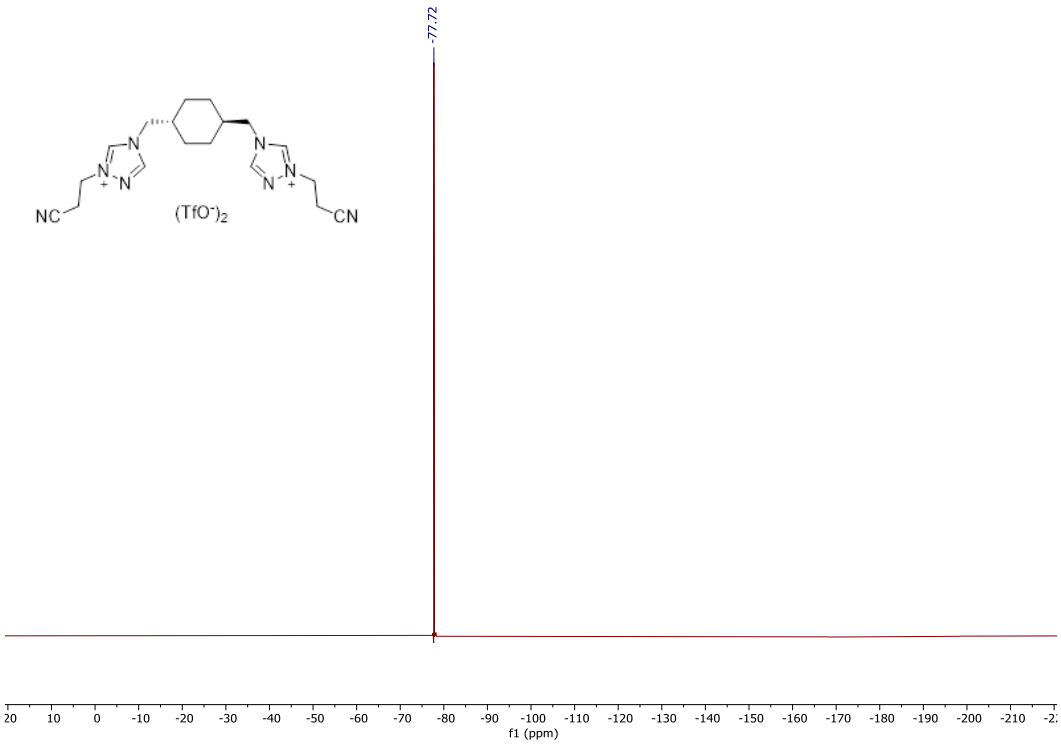

Fig. S7. ^{19}F NMR spectrum of 4,4'-((*trans*-cyclohexane-1,4-diyl)bis(methylene))bis(1-(2-cyanoethyl)-4*H*-1,2,4-triazol-1-ium) triflate**, 2-2**, in DMSO-d_6

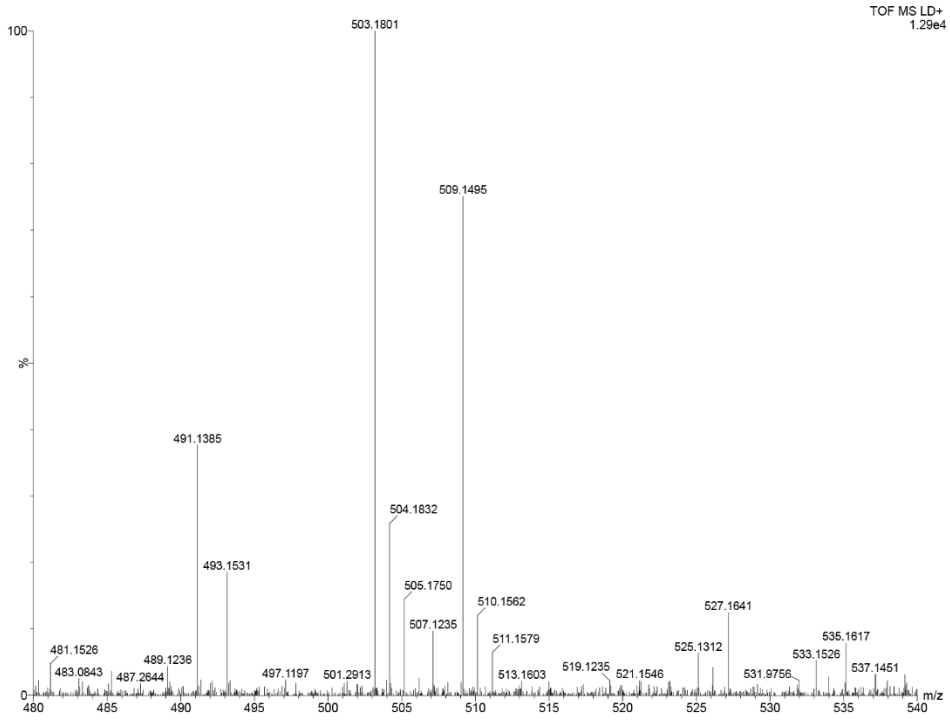

Fig. S8. MALDI-TOF mass spectrum of 4,4'-((*trans*-cyclohexane-1,4-diyl)bis(methylene))bis(1-(2-cyanoethyl)-4*H*-1,2,4-triazol-1-ium) triflate**, 2-2**

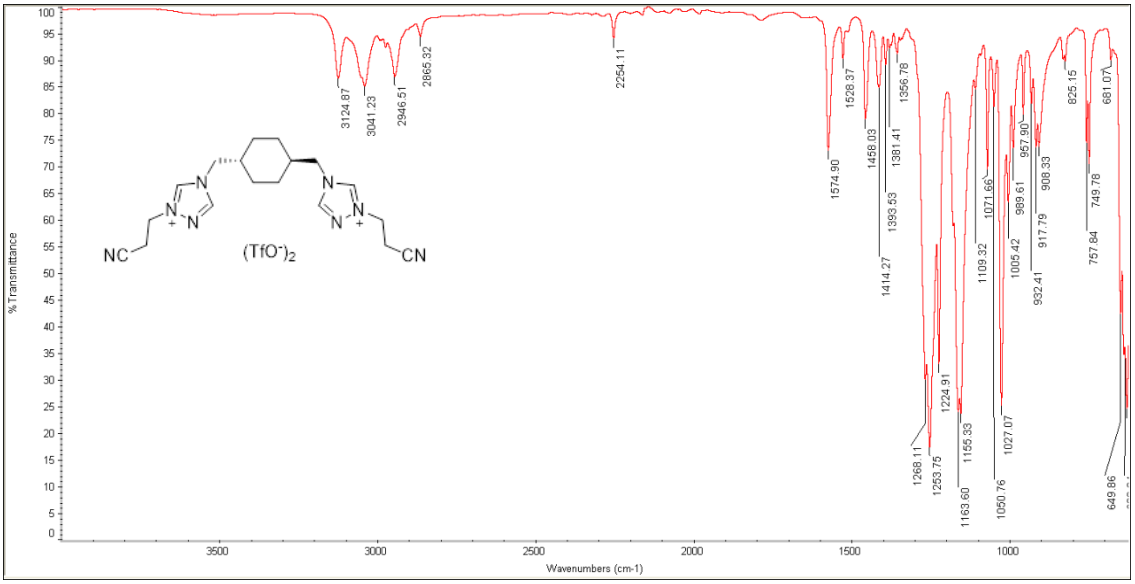

Fig. S9. IR spectrum of 4,4'-(((*trans*-cyclohexane-1,4-diyl)bis(methylene))bis(1-(2-cyanoethyl)-4*H*-1,2,4-triazol-1-ium) triflate**, 2-2**

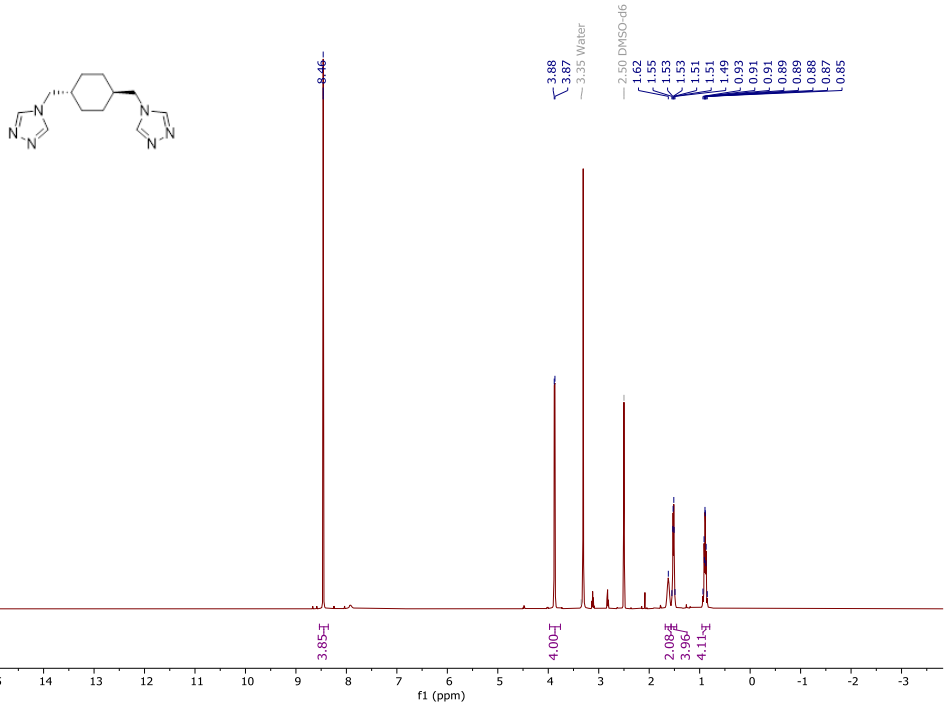

Fig. S10. ^{1}H NMR spectrum of *trans*-1,4-bis((4*H*-1,2,4-triazol-4-yl)methyl)cyclohexane, **L2**, in DMSO-d_6

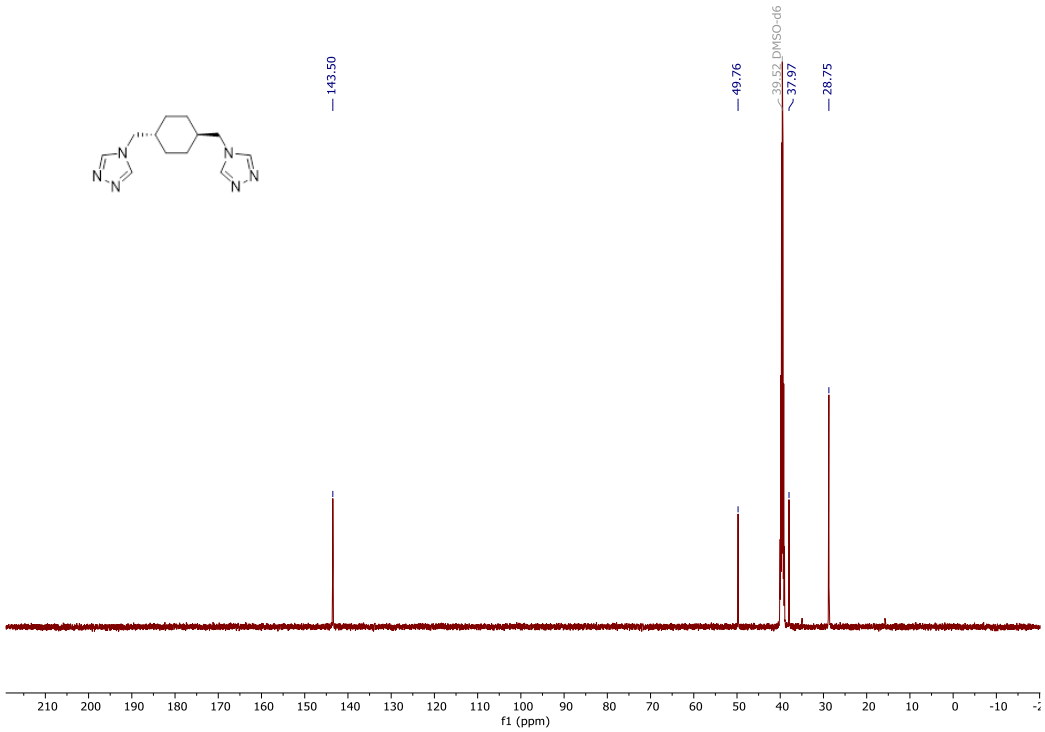

Fig. S11. ^{13}C NMR spectrum of *trans*-1,4-bis((4*H*-1,2,4-triazol-4-yl)methyl)cyclohexane, **L2**, in DMSO-d_6

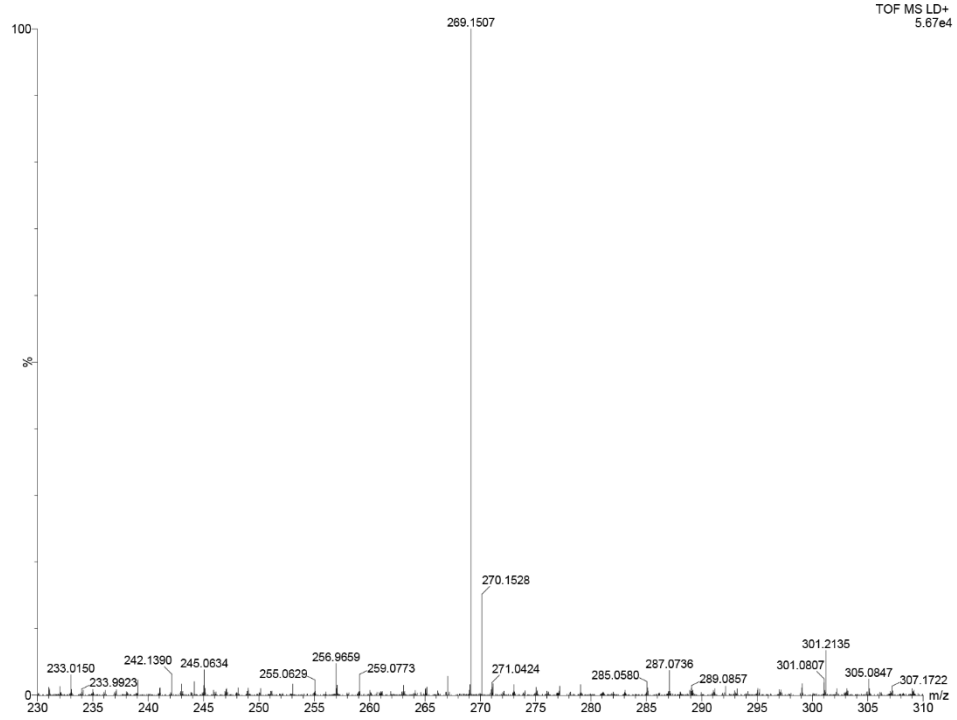

Fig. S12. MALDI-TOF mass spectrum of *trans*-1,4-bis((4*H*-1,2,4-triazol-4-yl)methyl)cyclohexane, **L2**

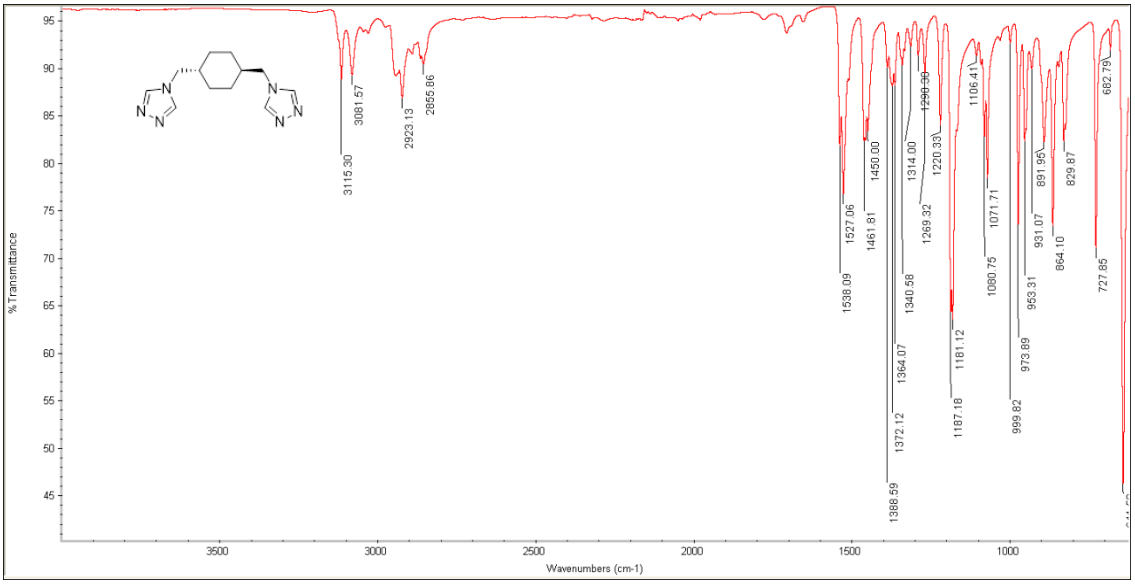

Fig. S13. IR spectrum of *trans*-1,4-bis((4*H*-1,2,4-triazol-4-yl)methyl)cyclohexane, **L2**

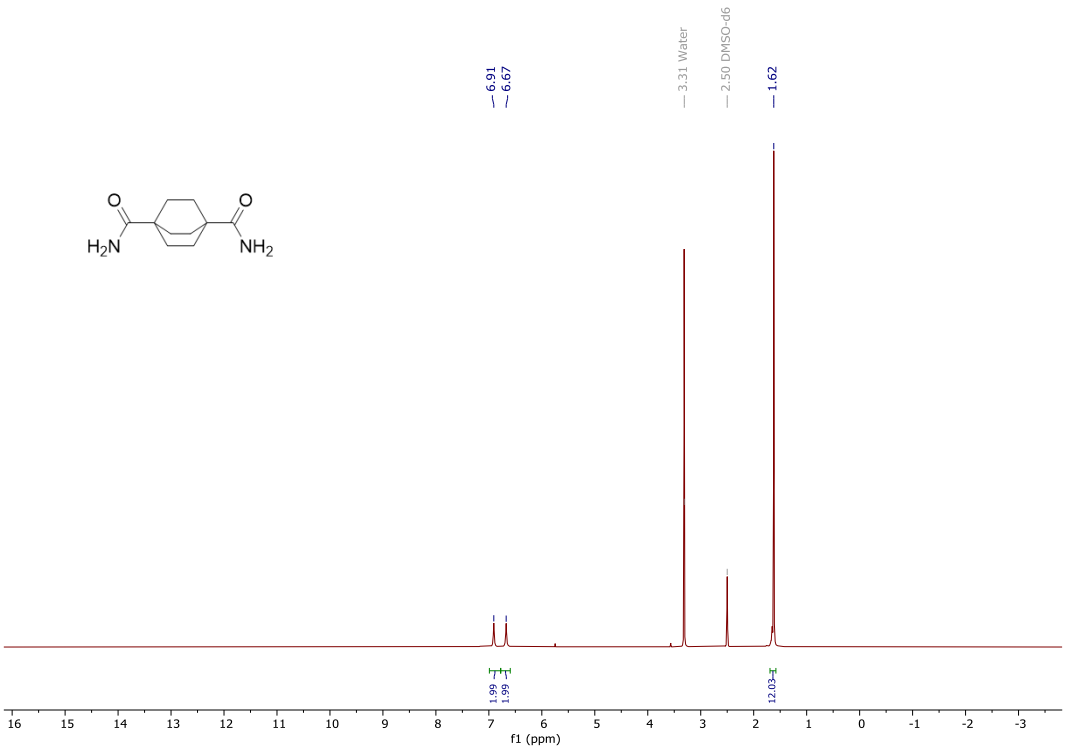

Fig. S14. ^{1}H NMR spectrum of bicyclo[2.2.2]octane-1,4-dicarboxamide, **3-1**, in DMSO-d_6

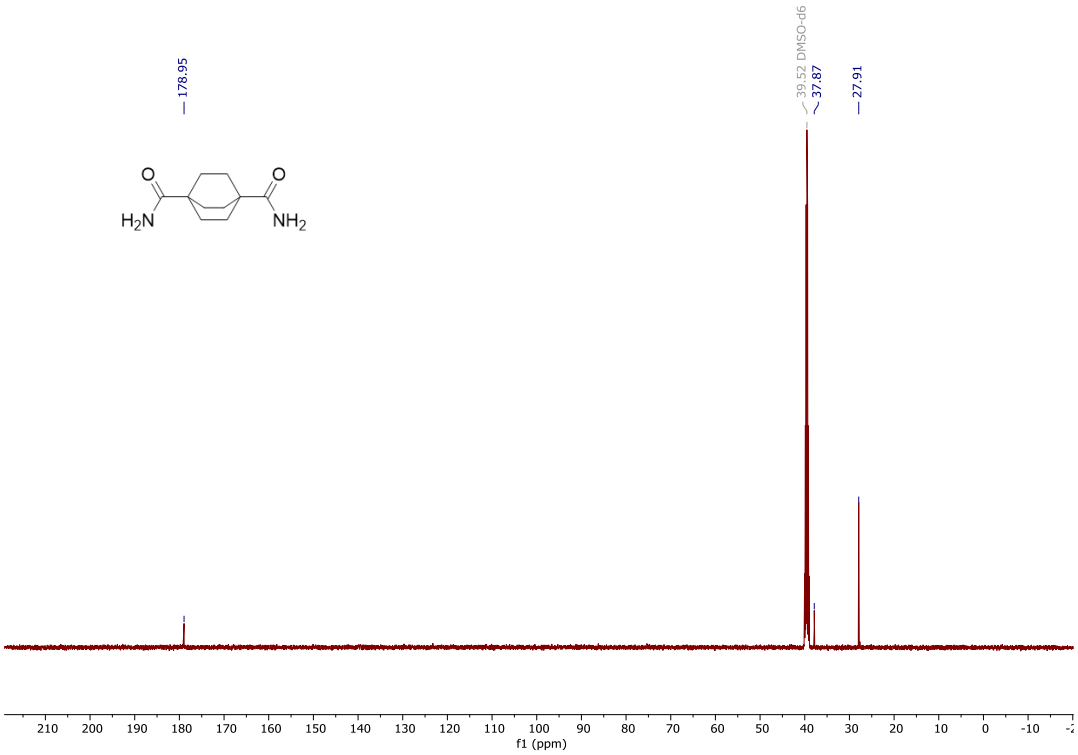

Fig. S15. ^{13}C NMR spectrum of bicyclo[2.2.2]octane-1,4-dicarboxamide, **3-1**, in DMSO-d_6

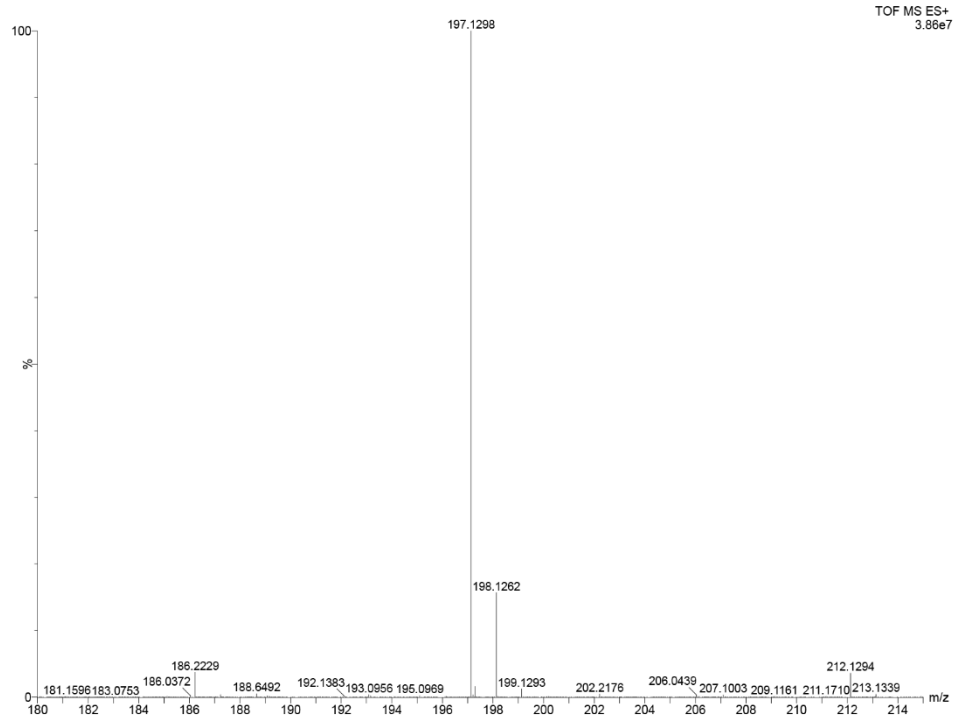

Fig. S16. MALDI-TOF mass spectrum of bicyclo[2.2.2]octane-1,4-dicarboxamide, **3-1**

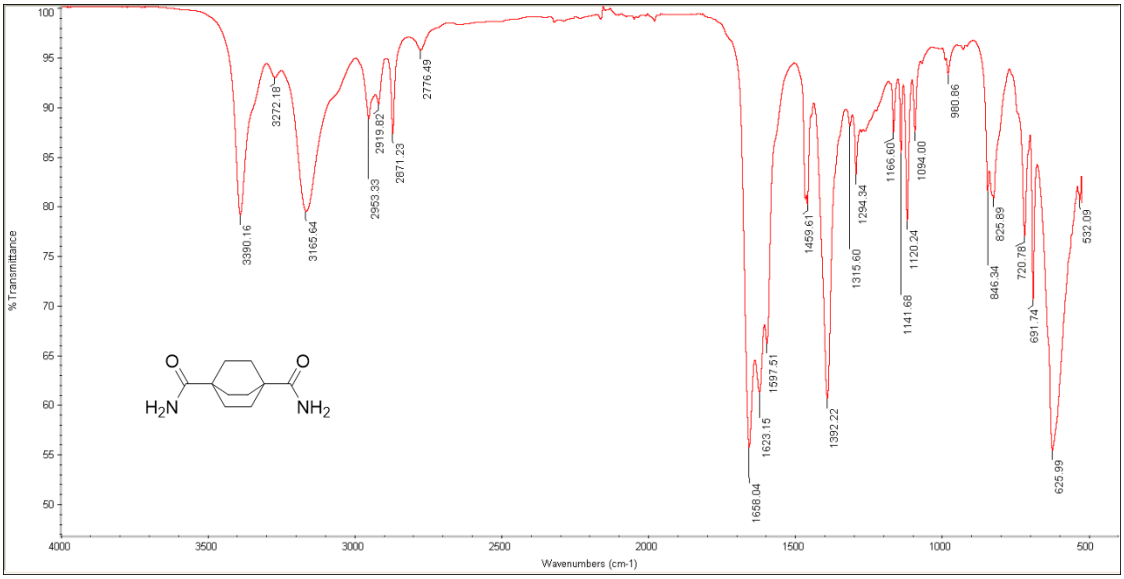

Fig. S17. IR spectrum of bicyclo[2.2.2]octane-1,4-dicarboxamide, **3-1**, in DMSO-d_6

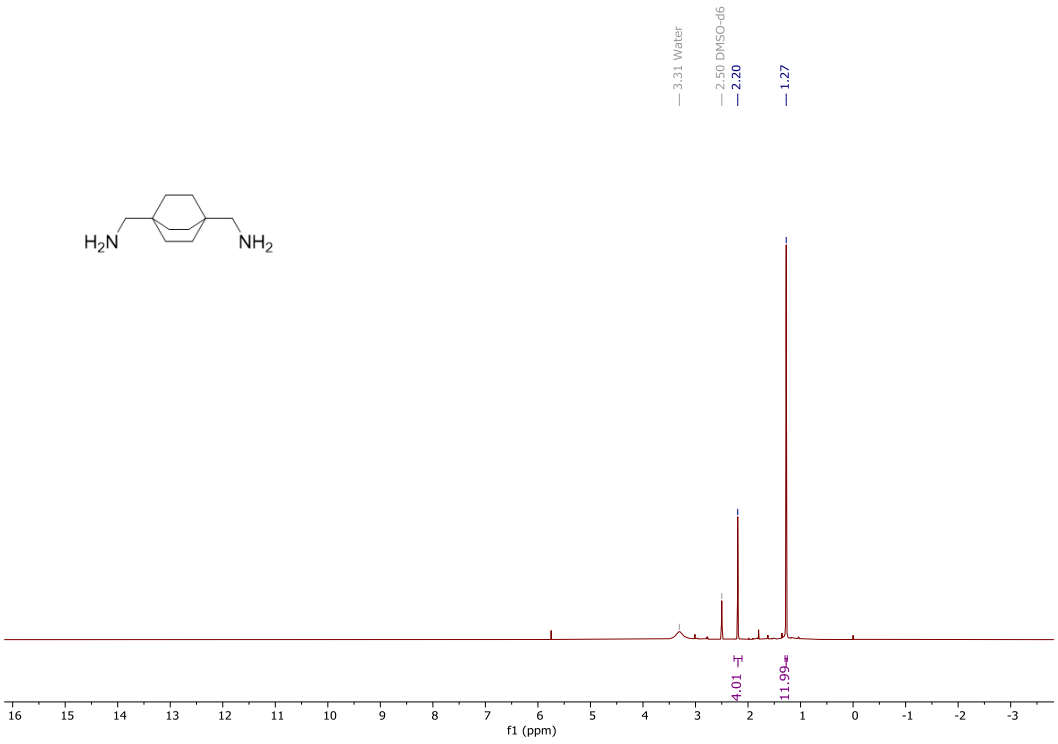

Fig. S18. ^{1}H NMR spectrum of bicyclo[2.2.2]octane-1,4-diyldimethanamine, **3-2**, in DMSO-d_6

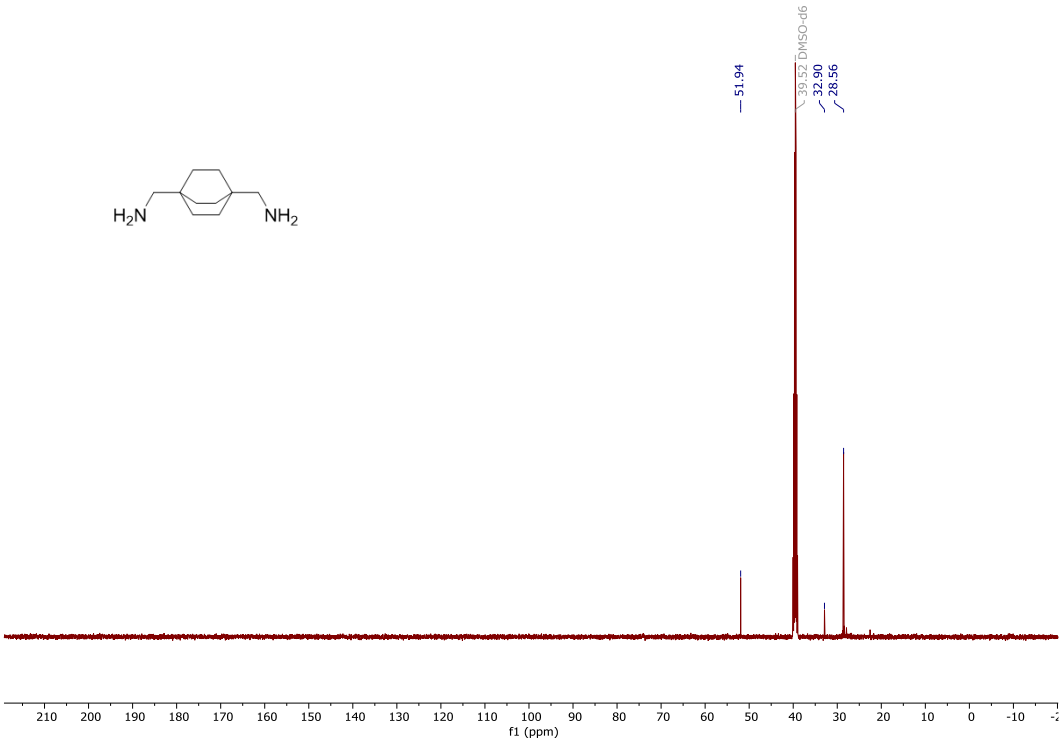

Fig. S19. ^{13}C NMR spectrum of bicyclo[2.2.2]octane-1,4-diyldimethanamine, **3-2**, in DMSO-d_6

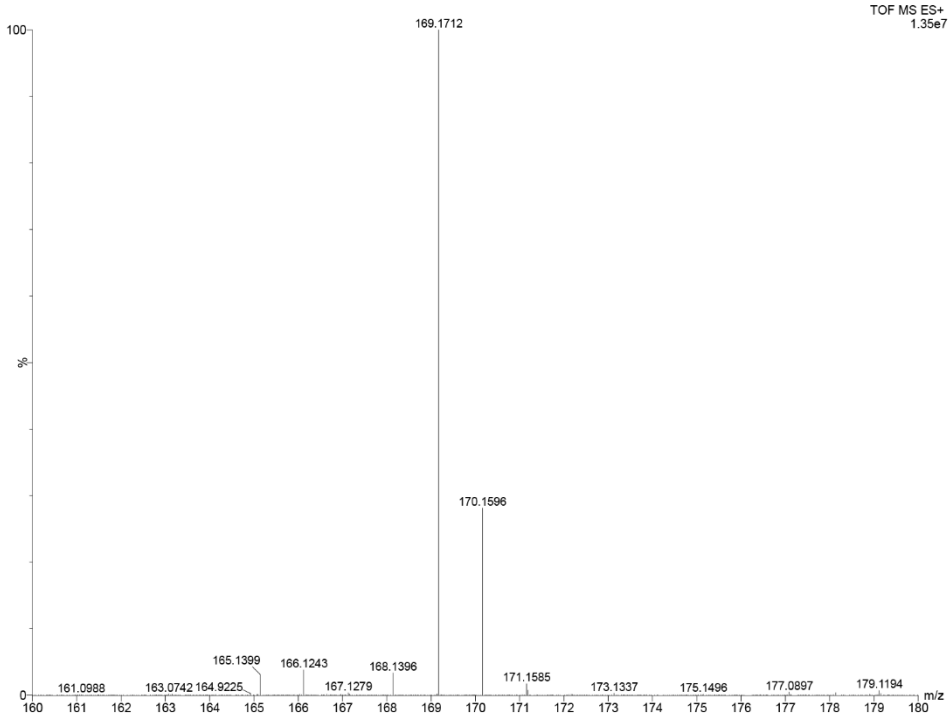

Fig. S20. MALDI-TOF mass spectrum of bicyclo[2.2.2]octane-1,4-diyldimethanamine, **3-2**

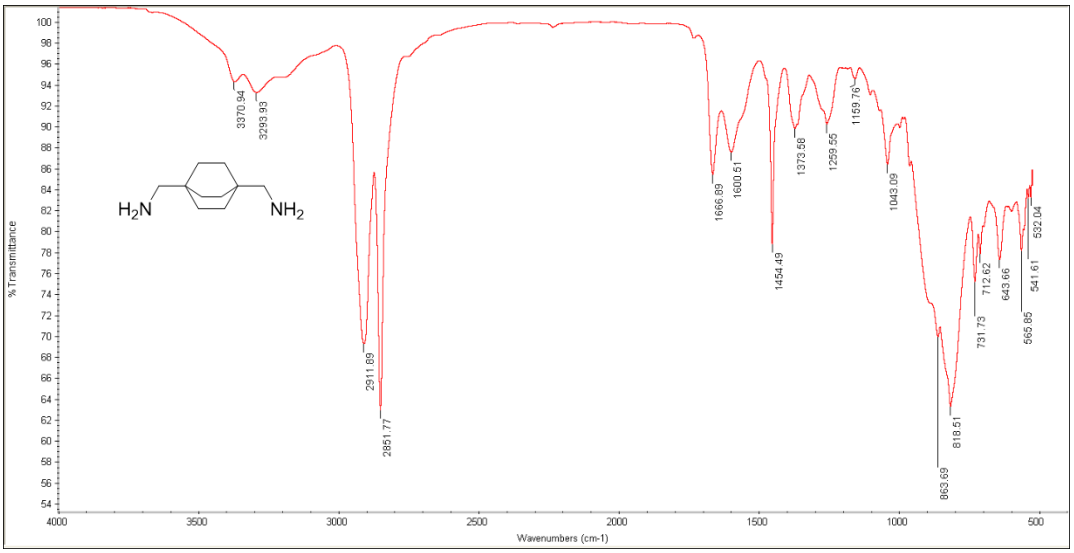

Fig. S21. IR spectrum of bicyclo[2.2.2]octane-1,4-diyldimethanamine, **3-2**

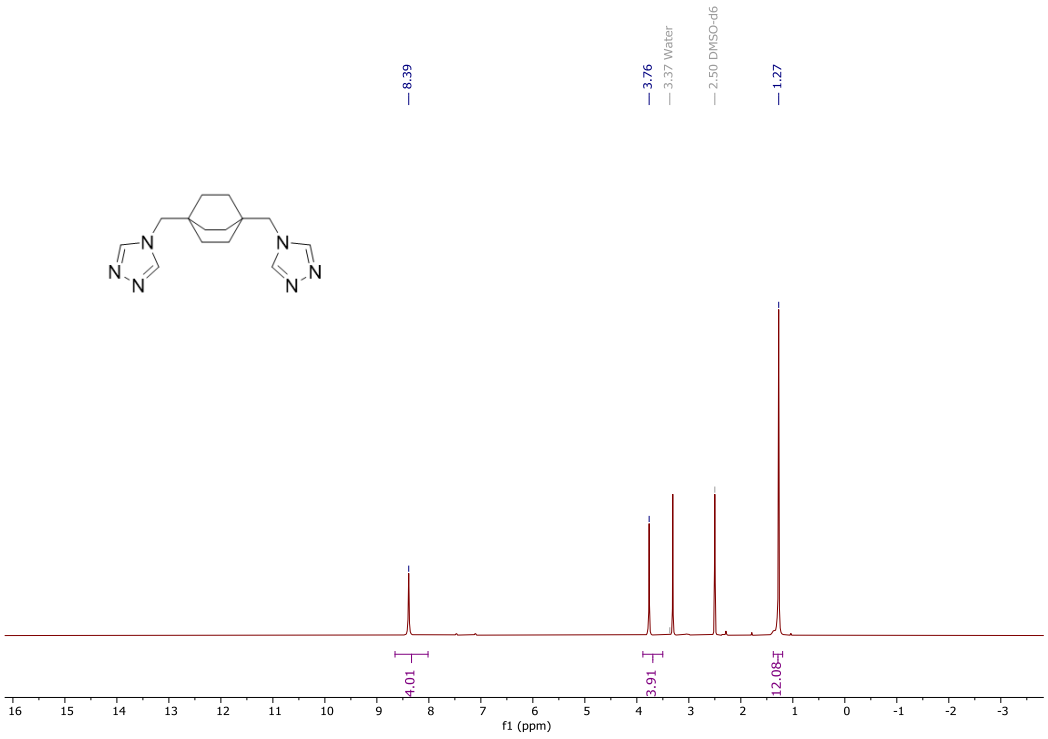

Fig. S22. ^{1}H NMR spectrum of 1,4-bis((4*H*-1,2,4-triazol-4-yl)methyl)bicyclo[2.2.2]octane, **L3**, in DMSO-d_6

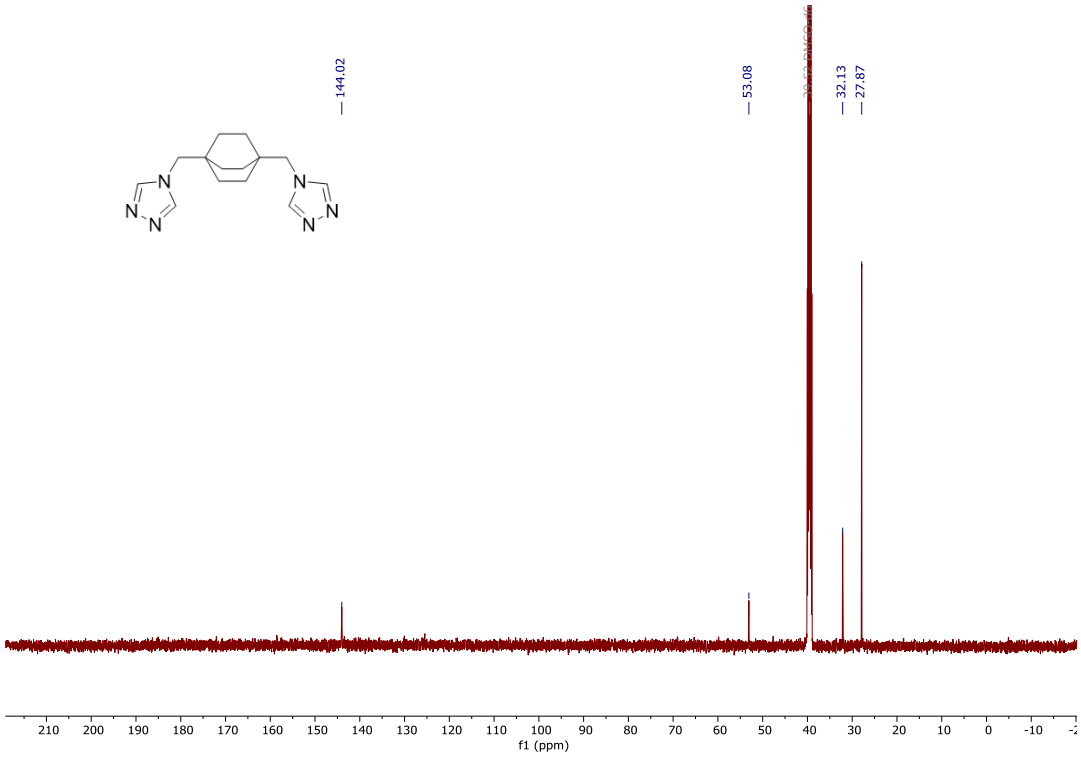

Fig. S23. ^{13}C NMR spectrum of 1,4-bis((4*H*-1,2,4-triazol-4-yl)methyl)bicyclo[2.2.2]octane, **L3**, in DMSO-d_6

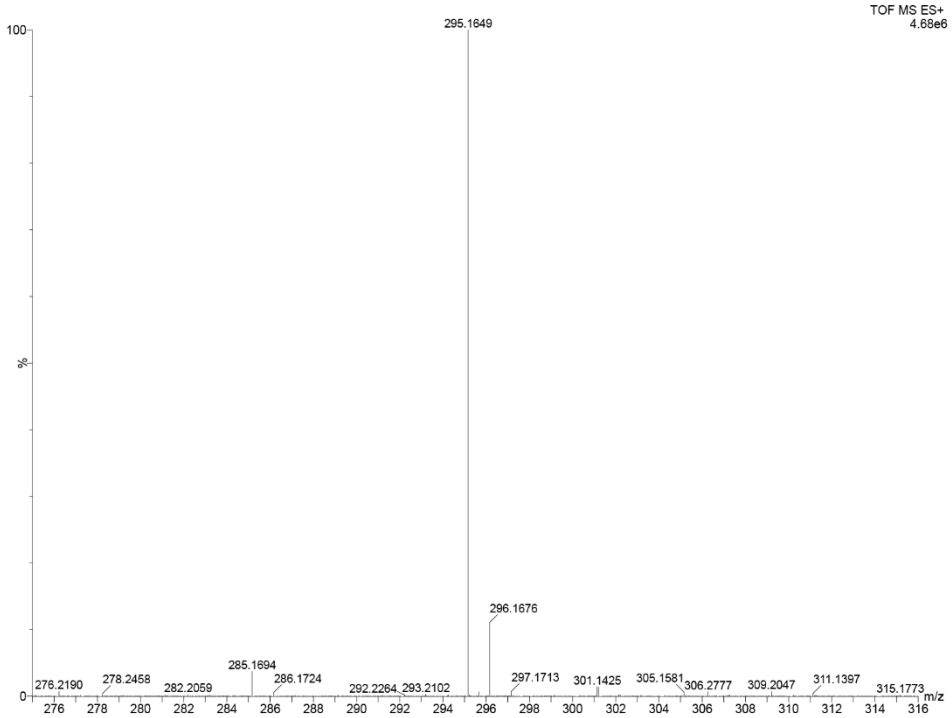

Fig. S24. MALDI-TOF mass spectrum of 1,4-bis((4*H*-1,2,4-triazol-4-yl)methyl)bicyclo[2.2.2]octane, **L3**

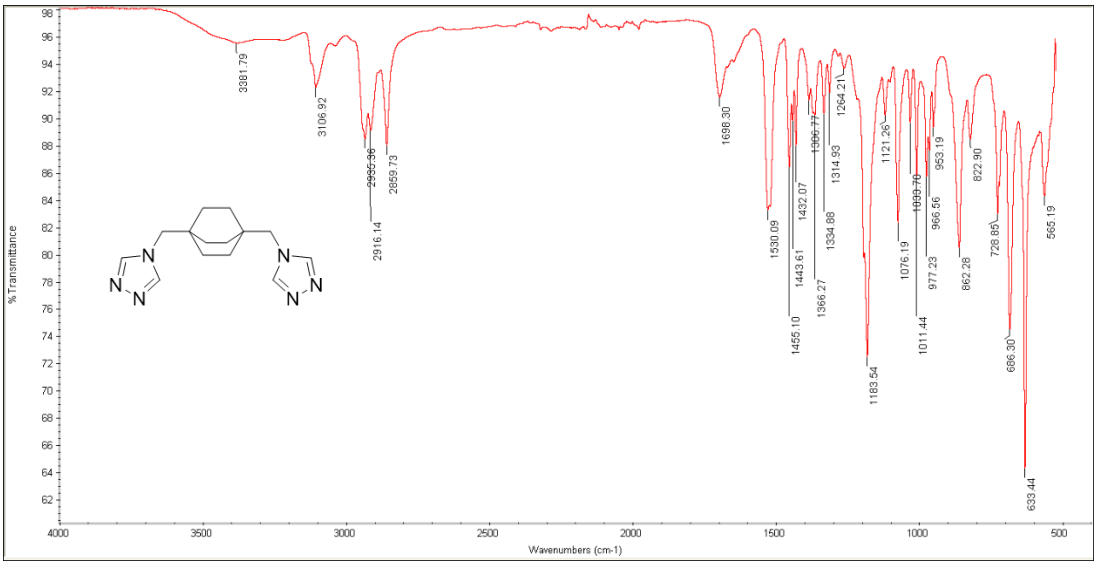

Fig. S25. IR spectrum of 1,4-bis((4*H*-1,2,4-triazol-4-yl)methyl)bicyclo[2.2.2]octane, **L3**

Characterization data of Ag(L2)(NO_3) and Ag_2(L3)(NO_3)$_2$

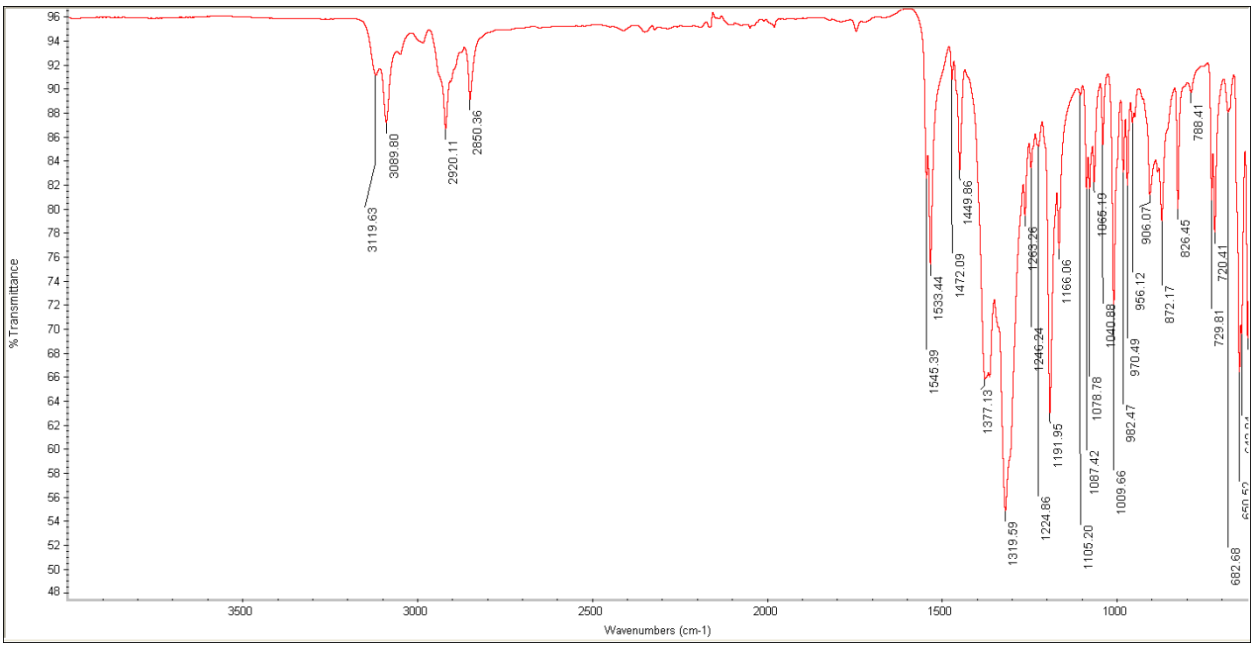

Fig. S26. IR spectrum of compound Ag(**L2**)(NO_3)

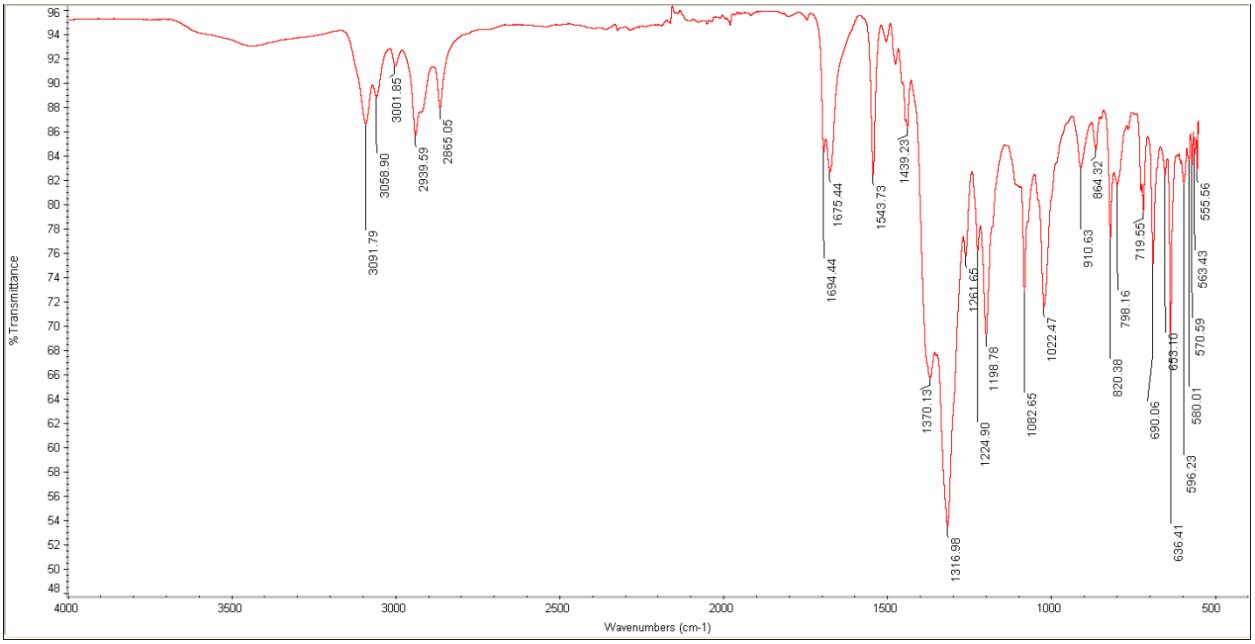

Fig. S27 IR spectrum of compound Ag_2(**L3**)(NO_3)$_2$

II. Single crystal X-ray diffraction data

Table S1. Single crystal structure parameters of compound **2-1**, **2-2**, **L2**, and **L3**

Compound	**2-1**	**2-2**	**L2**	**L3**
Empirical formula	$C_{10}H_{14}F_6O_6S_2$	$C_{20}H_{26}F_6N_8O_6S_2$	$C_{12}H_{18}N_6$	$C_{14}H_{20}N_6$
Formula weight	408.33	652.61	246.32	272.36
Temperature/K	100	100	100	100
Crystal system	monoclinic	triclinic	monoclinic	orthorhombic
Space group	*C2/c*	*P*-1	$P2_1/n$	$Pna2_1$
a/Å b/Å c/Å	15.4247(6) 9.6024(4) 10.6881(5)	6.6612(6) 7.0920(7) 15.1212(15)	8.4768(17) 10.883(2) 13.588(3)	12.7466(10) 17.0131(12) 6.1821(4)
α/° β/° γ/°	90 98.793(2) 90	94.455(4) 98.312(3) 90.959(4)	90 92.070(7) 90	90 90 90
Volume/Å^3	1564.45(12)	704.42(12)	1252.7(4)	1340.65(17)
Z	4	1	4	4
ρ_{calc}g/cm^3	1.734	1.538	1.306	1.349
μ/mm^{-1}	0.433	0.280	0.085	0.087
F(000)	832.0	336.0	528.0	584.0
Crystal size/mm^3	0.696 × 0.193 × 0.177	0.265 × 0.089 × 0.028	0.679 × 0.302 × 0.058	0.348 × 0.025 × 0.025
Radiation	MoKα (λ= 0.71073)	MoKα (λ = 0.71073)	MoKα (λ= 0.71073)	MoKα (λ = 0.71073)
2θ range for data collection/°	5.014 to 54.478	5.464 to 52.042	4.796 to 51.36	4.788 to 52.03
Index ranges	-19 ≤ h ≤ 19 -12 ≤ k ≤ 12 -13 ≤ l ≤ 13	-8 ≤ h ≤ 8, -8 ≤ k ≤ 8, -18 ≤ l ≤ 18	-10 ≤ h ≤ 10 -13 ≤ k ≤ 13 -16 ≤ l ≤ 16	-15 ≤ h ≤ 15, -20 ≤ k ≤ 20, -7 ≤ l ≤ 6
Reflections collected	16130	18304	30074	14888
Independent reflections	1759 [R_{int} = 0.0320, R_{sigma} = 0.0165]	2773 [R_{int} = 0.0794, R_{sigma} = 0.0479]	2378 [R_{int} = 0.0539, R_{sigma} = 0.0234]	2425 [R_{int} = 0.0811, R_{sigma} = 0.0558]
Data/restraints/parameters	1759/0/109	2773/0/190	2378/0/163	2425/1/181
Goodness-of-fit on F^2	1.094	1.049	1.136	1.082
Final R indexes [I>=2σ (I)]	R_1 = 0.0250, wR_2 = 0.0627	R_1 = 0.0470, wR_2 = 0.1156	R_1 = 0.0403, wR_2 = 0.0953	R_1 = 0.0649, wR_2 = 0.1183
Final R indexes [all data]	R_1 = 0.0280, wR_2 = 0.0642	R_1 = 0.0558, wR_2 = 0.1208	R_1 = 0.0464, wR_2 = 0.0981	R_1 = 0.0831, wR_2 = 0.1250
Largest diff. peak/hole / e Å^{-3}	0.36/-0.34	0.70/-0.48	0.20/-0.27	0.20/-0.24

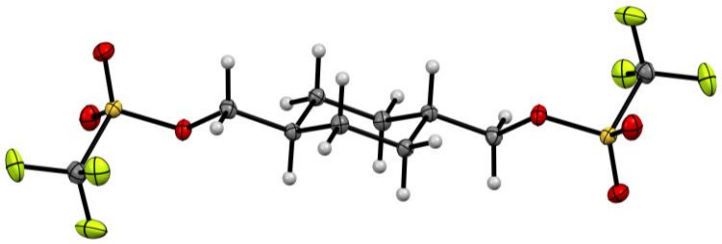

Fig. S28. ORTEP drawing of compound **2-1** showing thermal ellipsoids at the 50% probability level. The color scheme used: C grey, H white, O red, F green, and S yellow.

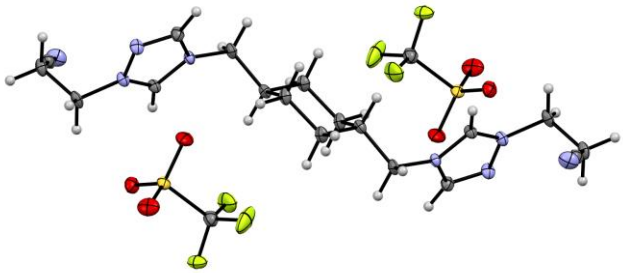

Fig. S29. ORTEP drawing of compound **2-2** showing thermal ellipsoids at the 50% probability level. The color scheme used: C grey, H white, N blue, O red, F green, and S yellow.

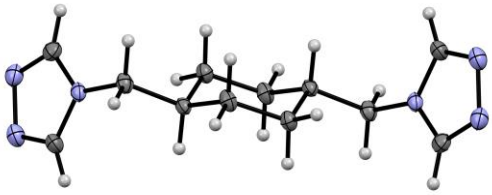

Fig. S30. ORTEP drawing of compound **L2** showing thermal ellipsoids at the 50% probability level. The color scheme used: C grey, H white, and N blue.

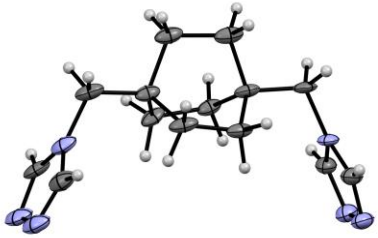

Fig. S31. ORTEP drawing of compound **L3** showing thermal ellipsoids at the 50% probability level. The color scheme used: C grey, H white, and N blue.

Table S2. Single crystal structure parameters of Ag(**L2**)(NO_3) and Ag_2(**L3**)(NO_3)$_2$

Compound	**Ag(L2)(NO_3)**	**Ag_2(L3)(NO_3)$_2$**
Empirical formula	$C_{12}H_{18}AgN_7O_3$	$C_7H_{10}AgN_4O_3$
Formula weight	416.20	306.06
Temperature/K	100	100
Crystal system	monoclinic	monoclinic
Space group	$P2_1/c$	C2/c
a/Å b/Å c/Å	12.5507(4) 12.9070(5) 9.9446(4)	22.261(3) 14.2526(16) 7.7279(11)
α/° β/° γ/°	90 108.3360(10) 90	90 108.177(5) 90
Volume/Å^3	1529.15(10)	2329.6(5)
Z	4	8
ρ_{calc}g/cm^3	1.808	1.745
μ/mm^{-1}	1.346	1.725
F(000)	840.0	1208.0
Crystal size/mm^3	0.2 × 0.108 × 0.048	0.154 × 0.042 × 0.039
Radiation	MoKα (λ = 0.71073)	MoKα (λ = 0.71073)
2θ range for data collection/°	4.652 to 55.746	5.716 to 52.868
Index ranges	-16 ≤ h ≤ 16, -16 ≤ k ≤ 16, -13 ≤ l ≤ 13	-27 ≤ h ≤ 26, 0 ≤ k ≤ 17, 0 ≤ l ≤ 9
Reflections collected	40709	2361
Independent reflections	3646 [R_{int} = 0.0321, R_{sigma} = 0.0142]	2361 [R_{int} = 0.0772, R_{sigma} = 0.0678]
Data/restraints/parameters	3646/0/235	2361/0/118
Goodness-of-fit on F^2	1.031	1.082
Final R indexes [I>=2σ (I)]	R_1 = 0.0172, wR_2 = 0.0399	R_1 = 0.0893, wR_2 = 0.2077
Final R indexes [all data]	R_1 = 0.0202, wR_2 = 0.0415	R_1 = 0.1131, wR_2 = 0.2186
Largest diff. peak/hole / e Å^{-3}	0.37/-0.41	3.29/-2.50

III. Powder X-ray diffraction data

PXRD data compound Ag(**L2**)(NO_3) and Ag_2(**L3**)(NO_3)$_2$

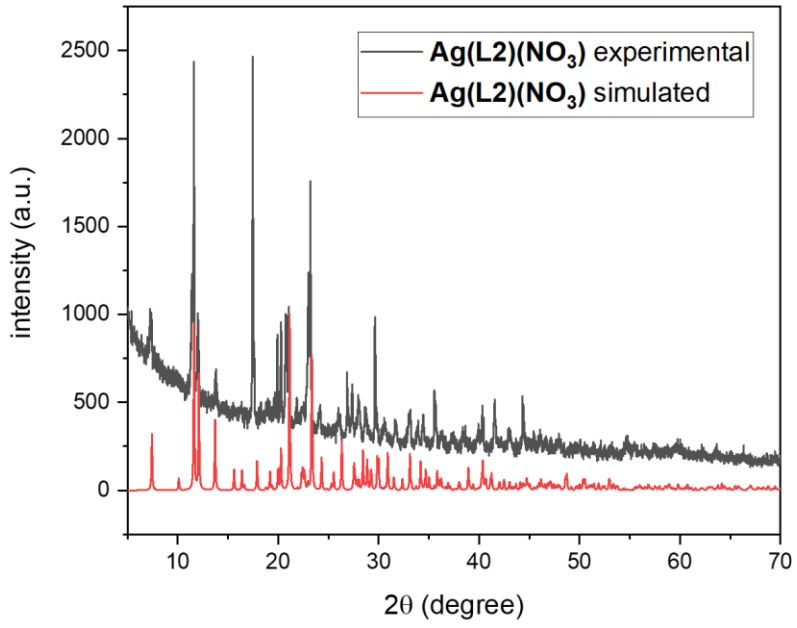

Fig. S32. PXRD pattern of Ag(**L2**)(NO_3)

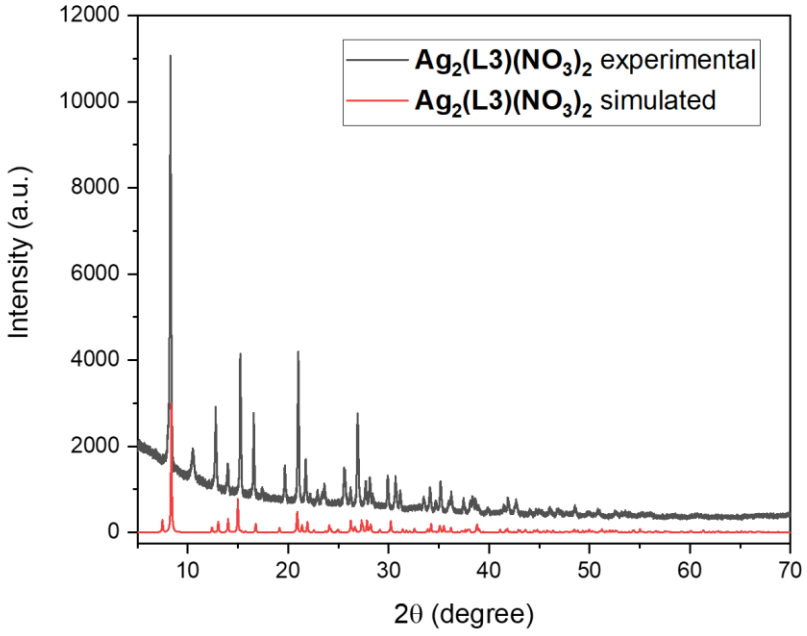

Fig. S33. PXRD pattern of Ag_2(**L3**)(NO_3)$_2$

IV. Hirshfeld surface analysis

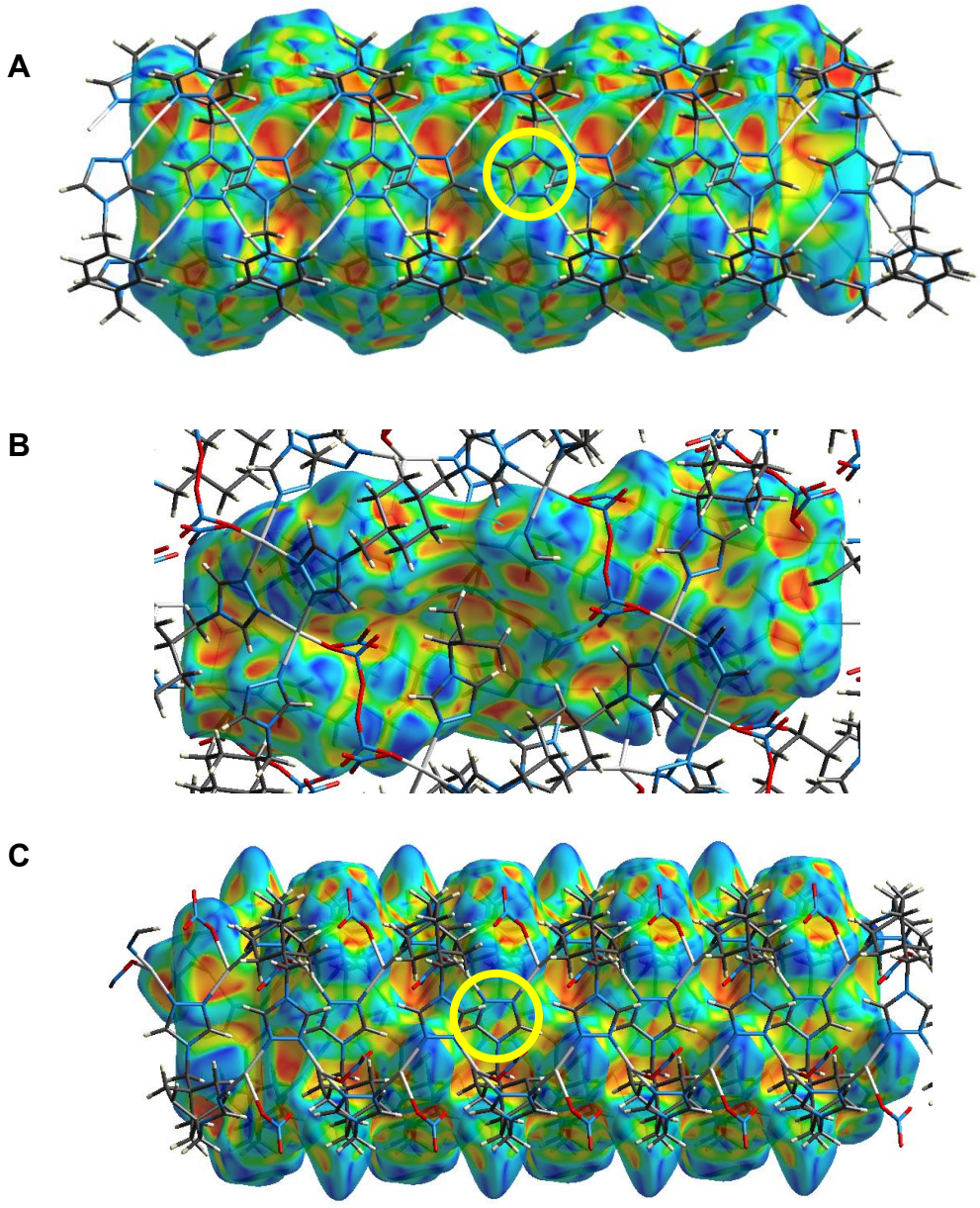

Fig. S34. Hirshfeld surface analysis of (A) Ag_2(**L1**)$(NO_3)_2$, (B) Ag(**L2**)(NO_3), and (C) Ag_2(**L3**)$(NO_3)_2$. Yellow circles indicate the area where π–π interaction between triazoles are observed with plane distances of 3.373(12) and 3.329(9) Å for Ag_2(**L1**)$(NO_3)_2$ and Ag_2(**L3**)$(NO_3)_2$, respectively.

V. References

1. A. Horváth, Synthesis, 1995, 1995, 1183-1189.
2. P. Bamborough, C.-w. Chung, R. C. Furze, P. Grandi, A.-M. Michon, R. J. Sheppard, H. Barnett, H. Diallo, D. P. Dixon, C. Douault, E. J. Jones, B. Karamshi, D. J. Mitchell, R. K. Prinjha, C. Rau, R. J. Watson, T. Werner and E. H. Demont, *Journal of Medicinal Chemistry*, 2015, **58**, 6151-6178.
3. S. M. Wilkinson, H. Gunosewoyo, M. L. Barron, A. Boucher, M. McDonnell, P. Turner, D. E. Morrison, M. R. Bennett, I. S. McGregor, L. M. Rendina and M. Kassiou, *ACS Chemical Neuroscience*, 2014, **5**, 335-339.
4. C. R. Murdock and D. M. Jenkins, *Journal of the American Chemical Society*, 2014, **136**, 10983-10988.